

Biocompatible coupling of therapeutic fusion proteins to human erythrocytes

Carlos H. Villa,^{1,2} Daniel C. Pan,² Ian H. Johnston,^{2,3} Colin F. Greineder,² Landis R. Walsh,² Elizabeth D. Hood,² Douglas B. Cines,¹ Mortimer Poncz,³ Don L. Siegel,¹ and Vladimir R. Muzykantov²

¹Department of Pathology and Laboratory Medicine and ²Department of Systems Pharmacology and Translational Therapeutics, Perelman School of Medicine, University of Pennsylvania, Philadelphia, PA; and ³Division of Pediatric Hematology, Children's Hospital of Philadelphia, Philadelphia, PA

Key Points

- Thrombomodulin was fused to scFvs targeting RhCE (Rh17 epitope) and band 3/GPA (Wr^b epitope).
- Fusion proteins were efficacious in a humanized microfluidic model of inflammatory thrombosis.

Carriage of drugs by red blood cells (RBCs) modulates pharmacokinetics, pharmacodynamics, and immunogenicity. However, optimal targets for attaching therapeutics to human RBCs and adverse effects have not been studied. We engineered nonhuman-primate single-chain antibody fragments (scFvs) directed to human RBCs and fused scFvs with human thrombomodulin (hTM) as a representative biotherapeutic cargo (hTM-scFv). Binding fusions to RBCs on band 3/glycophorin A (GPA; Wright b [Wr^b] epitope) and RhCE (Rh17/Hr0 epitope) similarly endowed RBCs with hTM activity, but differed in their effects on RBC physiology. scFv and hTM-scFv targeted to band 3/GPA increased membrane rigidity and sensitized RBCs to hemolysis induced by mechanical stress, while reducing sensitivity to hypo-osmotic hemolysis. Similar properties were seen for other ligands bound to GPA and band 3 on human and murine RBCs. In contrast, binding of scFv or hTM-scFv to RhCE did not alter deformability or sensitivity to mechanical and osmotic stress at similar copy numbers bound per RBCs. Contrasting responses were also seen for immunoglobulin G antibodies against band 3, GPA, and RhCE. RBC-bound hTM-scFv generated activated protein C (APC) in the presence of thrombin, but RhCE-targeted hTM-scFv demonstrated greater APC generation per bound copy. Both Wr^b- and RhCE-targeted fusion proteins inhibited fibrin deposition induced by tumor necrosis factor- α in an endothelialized microfluidic model using human whole blood. RhCE-bound hTM-scFv more effectively reduced platelet and leukocyte adhesion, whereas anti-Wr^b scFv appeared to promote platelet adhesion. These data provide a translational framework for the development of engineered affinity ligands to safely couple therapeutics to human RBCs.

Introduction

Drug delivery by red blood cells (RBCs) was envisioned decades ago¹⁻³ and the field has seen substantial growth,⁴⁻⁶ spurred by advances in drug loading within cells,^{7,8} approaches to coupling to the cell surface,^{9,10} new technologies for genetic manipulation,¹¹ and clinical successes in cellular therapeutics overall.¹² Delivery by carrier RBCs enhances pharmacokinetics and, in some cases, the pharmacodynamics of the loaded agents. Furthermore, recent reports that RBCs can modulate immunogenicity, even inducing tolerance, expand the potential applications of RBC delivery.¹³⁻¹⁵ RBC-encapsulated agents, including dexamethasone and L-asparaginase, have entered clinical trials.

Surface coupling may offer advantages with respect to clinical translatability, manufacturing, and biocompatibility.¹⁶ Animal studies demonstrated highly desirable features of surface-coupled antithrombotic

and anti-inflammatory agents.^{10,17-20} For example, coupling of thrombomodulin (TM) to murine RBCs improves its efficacy in thrombotic,²⁰ inflammatory, and ischemia-reperfusion injuries.²¹ Previous reports have generally used fusion proteins, antibodies, and peptides to couple therapeutics to the surface of murine and porcine, but not human, RBCs. Coupling to murine RBCs is typically accomplished by derivatives of Ter119, an antibody to an epitope associated with glycophorin A (GPA),²² or with ERY1 peptide, whose putative target is GPA.¹³ Although no overt adverse effects on RBCs have been noted when using these ligands,²³ the effects of their binding to murine RBCs have not been characterized extensively.

RBC ligands, even monovalent, specifically targeted to GPA and band 3, have the potential to cause undesirable alterations of RBC, including changes in deformability,²⁴⁻²⁸ exposure of phosphatidylserine (PS),²⁹ and generation of reactive oxygen species (ROS).³⁰ Although antibodies to GPA and band 3 generally reduce membrane deformability, in early studies of the membrane deformability of antibody-coated RBCs, others observed that for some antigens, nonspherocytic antibody-sensitized RBCs could maintain normal deformability.³¹ Membrane effects vary even among epitopes within the same target protein. Surface proteins may have important intrinsic roles that could be disrupted by ligand binding, such as GPA interaction with neutrophils to promote quiescence³² or ion transport by band 3.³³ It is critical to examine untoward effects to identify optimal RBC targets. The ideal target should be erythroid specific, present in sufficient copy number for its therapeutic intent, be widely distributed among human populations, and for most applications, not compromise RBC biocompatibility. Importantly, expression of 3 blood group systems is largely confined to erythropoiesis, GPA (MNS system), band 3 (Diego system), and Rhesus family members (RhCE and RhD; Rh system).³⁴

To address these questions, we identified single-chain antibody fragments (scFvs) against epitopes on band 3/GPA protein complexes (Wright b [Wr^b] and RhCE protein (Rh17/Hr₀)) on human erythrocytes using antibody phage-display libraries prepared from immunized cynomolgus macaques (*Macaca fascicularis*). Both antigens are present on RBCs from nearly 100% of the population and are considered erythroid specific.^{35,36} Although targeting Wr^b can induce rigidity,²⁸ ligands to RhCE determinants have not been extensively characterized on human RBCs with respect to effects on red cell physiology. These antibodies were fused to the extracellular domain of human TM (hTM-scFv) to produce a multifaceted thromboprophylactic agent.²⁰ We characterized the binding of the scFv and hTM-scFv and compared how both affected several clinically relevant aspects of human RBC physiology, including osmotic resistance, mechanical strength, deformability under flow, and exposure of surface PS. The efficacy of these human RBC-coupled TMs was compared using a whole-blood, microfluidic model of inflammatory thrombosis recently described by our group.³⁷

Materials and methods

Red blood cells

Human whole blood was obtained from healthy volunteer donors. All studies involving human subjects were approved by the institutional review board of the University of Pennsylvania. Written informed consent was obtained and phlebotomy was performed via the antecubital veins using a 21-gauge butterfly needle. Specimens were drawn into 3.2% sodium citrate vacuum tubes (BD, Franklin

Lakes, NJ). To obtain RBCs for ektacytometry and cell-binding studies, whole blood was spun at 1000g for 10 minutes and the plasma and buffy coat were discarded. A portion of the packed red cells was then resuspended in balanced salt solution (phosphate-buffered saline [PBS] or Hank-buffered salt solution [HBSS]) with calcium and magnesium and 2% normal human AB serum (Sigma-Aldrich, St. Louis, MO) at the indicated hematocrit for each subsequent assay. In assays of osmotic resistance and mechanical resistance, human RBCs were isolated from the retained segments of nonexpired (<21-day-old) O⁺, leukoreduced, irradiated RBCs from our hospital blood bank and prepared similarly. In these assays, similar results were seen using either fresh RBCs from volunteer donors or RBCs isolated from retained segments.

Derivation and production of antibodies and fusion proteins

An immunoglobulin G (IgG) Fab/phage-display library was prepared from the peripheral blood lymphocytes of a human erythrocyte hyperimmunized macaque using homologous human V-region oligonucleotides.³⁸ Fab/phage specific for human RBCs was isolated by panning on intact human RBCs. Monoclonal Fab/phage was grown to produce antibodies for immunoassays and their corresponding DNA was extracted for sequencing. To identify target epitopes, antibodies were screened against RBCs of known serologic phenotypes, including rare cells lacking highly conserved antigens, using standard immunohematologic agglutination techniques.³⁹

After identification of the target epitopes, clones reactive against Wr^b (aBand3/GPA epitope) and Rh17 (an RhCE epitope, also known as Hr⁰) present at the highest titers were chosen to produce scFv derivatives of the encoded antibodies. Sequences of the antibody clones examined herein are available in the supplemental Methods. For each heavy-chain variable region (VH) and light-chain variable region (VL), restriction enzyme sites were introduced for cloning into expression vectors and fusion to the extracellular domain of hTM (Glu22-Ser515) as previously described.²⁰ VH and VL were also ligated into a pBAD/gIII expression system (Thermo Fisher Scientific, Carlsbad, CA) to produce scFv alone in *Escherichia coli* periplasm. Sequences were modified by custom synthesis of double-stranded gene fragments (gBlock; IDT, Coralville, IA). Details of recombinant protein production can be found in the supplemental Methods.

Microfluidic assay

Microfluidic experiments were performed on a Bioflux 1000 multiwell microfluidic system (Fluxion Biosciences, San Francisco, CA). Microchannels were endothelialized with human umbilical vein endothelial cells as described previously,³⁷ which typically resulted in complete coverage of the microchannels. Channels were treated with tumor necrosis factor- α (TNF- α ; 10 ng/mL) under flow (at shear stress of 5 dyne/cm²) for 6 hours to flow condition and induce activation prior to exposure to whole blood. Whole blood was obtained from healthy volunteer donors and collected into citrate collection tubes containing corn trypsin inhibitor. The indicated concentrations of recombinant proteins were added to the whole blood for 1 hour prior to perfusion through the microchannels. Fluorescently labeled anti-fibrin antibodies and calcein AM were also added to blood 15 minutes before microfluidic assay to image fibrin deposition and leukocyte and platelet adhesion, respectively.

Blood was flowed through the channels under conditions mimicking postcapillary venules (5 dyne/cm²) for 20 minutes while images were continuously acquired. Controls and experimental conditions were compared on simultaneously run parallel channels using a motorized stage for real-time acquisition. Images were analyzed using ImageJ for quantification of mean fluorescence intensity.

Osmotic and mechanical resistance assays

Osmotic and mechanical resistance was measured as previously described.⁴⁰ In brief, human RBCs obtained from retained segments of donor RBCs were resuspended in PBS at 5% hematocrit prior to incubation with various concentrations of antibodies, antibody fragments, or fusion proteins. The RBCs were then washed and exposed to osmotic or mechanical stress. Osmotic stress was induced by incubation in various concentrations of buffered (10 mM phosphate) hypo-osmolar NaCl solution (0-308 mOsm total) for 5 minutes. The suspensions were then centrifuged at 13 400g and the resulting supernatants were assayed for hemoglobin content by measuring absorbance at 540 nm. Hemolysis of equivalent concentrations of RBCs in water was taken as 100% hemolysis. To measure mechanical stress, RBCs were similarly treated with antibodies and fusion proteins, resuspended at 1% hematocrit, and rotated in the presence of 8-mm × 4-mm glass beads (Corning Pyrex, Corning, NY) for 1 hour at 37°C. The RBC suspension supernatants were then similarly analyzed spectrophotometrically for hemolysis.

Ektacytometry

Ektacytometry was performed using a RheoScan AnD system (Rheo Meditech, Seoul, Republic of Korea). In a typical experiment, 50 μL of 5% RBCs or 5 μL of whole blood was resuspended in 700 μL of a 5.5% (wt/vol) solution of 360-kDa poly-vinylpyrrolidone (Sigma-Aldrich, St. Louis, MO) in PBS. A 500-μL sample within each microfluidic chamber was then analyzed per the manufacturer's protocol. The elongation indices at the corresponding shear stresses were then input into statistical software (Prism, GraphPad, San Diego, CA) and the data were fit using nonlinear regression and a Streekstra-Bronkhorst model⁴¹ to derive the maximal elongation indices (Elmax) and shear stress at half-maximal deformation (SS1/2).

Results

Synthesis of targeting ligands

Using antibody phage display, we identified nonhuman-primate Fab antibody fragments to antigenic determinants on human RBCs. By panning phage libraries on human RBCs, we produced a Fab/phage preparation with >10⁷ RBC-specific clones capable of agglutinating human RBCs. By performing binding assays against rare RBC types lacking highly conserved antigens and epitopes, we identified the target antigens of >30 of these clones. At least 34 clones bound the Wr^b epitope formed by a band 3/GPA interaction, present on the RBCs of essentially 100% of the human population. The Wr^b epitope, determined by the protein sequence of band 3, is a site of association between band 3 with GPA, and GPA expression is simultaneously required for its presence on the membrane.⁴² At least 3 other clones bound to a highly conserved epitope Rh17(Hr⁰) on human RhCE protein, also present on essentially 100% of the human population except for rare Rh_{null} or D phenotypes. Both of these targets are specific for erythroid lineage.^{34,42,43} We assessed the extent of humanness of the

variable chains using T20 scores⁴⁴; scores of 79.8 for VH and 93.5 for VL framework regions were calculated for the anti-Rh17 (aRh17), and 86.0 for VH and 85.4 for VL framework regions were calculated for anti-Wr^b (aWr^b). These scores are comparable with "humanized" antibodies⁴⁴ and therefore are encouraging with respect to potential lack of immunogenicity of derivatives of these ligands.

Binding of ligands and cargoes to RBCs

The sequences of the variable fragment genes were cloned into plasmids to produce scFvs of the parent Fab, as well as fusions of the scFv antibodies with hTM. These scFvs and hTM-scFvs were produced with high purity as characterized by sodium dodecyl sulfate gel electrophoresis and size-exclusion high-performance liquid chromatography (HPLC), with peaks consistent with the expected molecular weights (Figure 1A-B). We then performed direct binding assays with radiolabeled and fluorescently labeled scFv antibody fragments and fusion proteins (see supplemental Methods). The aRh17 and aWr^b scFvs and their corresponding TM fusions demonstrated similar binding affinities (equilibrium dissociation constant [*K_D*] 21-53 nM; Figure 1C-D; supplemental Table 2), as did both radioiodinated and fluorescently labeled proteins (supplemental Figure 1). The scFvs and fusion proteins bound to conserved epitopes on human, but not mouse, rat, or pig RBCs (supplemental Figure 1), and binding parameters (*K_D*, maximum number of binding sites [B_{max}]) were consistent between multiple donors. Binding saturated at the expected level of target expression (B_{max} of 100 000 to 160 000 copies per RBC for aRh17 and 750 000 to 900 000 copies per RBC for aWr^b).⁴⁵ The dissociation rates were similar for both scFvs alone and their corresponding fusions, with >50% of the ligands remaining bound after 4 hours at 37° (Figure 1E-F; supplemental Table 2). We also examined effects of shear stress on scFv binding and the potential for ligand exchange onto unbound RBCs in whole blood under constant mixing (supplemental Figures 2 and 3). These experiments demonstrated that short periods of low (5 dyne/cm²) and high (200 dyne/cm²) shear in whole blood did not alter scFv binding, and that similar dissociation kinetics were seen in the presence of whole blood containing mostly unbound RBCs (with gradual exchange onto the unbound RBC population). Hemagglutination by an anti-TM secondary antibody was seen when hTM-scFv fusions were added at concentrations estimated to generate ~1000 copies of TM per RBC based on the calculated affinities (Figure 1G). The fusion proteins alone did not induce aggregation or agglutination of RBCs in the absence of secondary anti-TM. Morphology of fusion protein-loaded RBCs was confirmed on Wright-Giemsa-stained peripheral blood smears and no morphologic abnormalities in the RBCs were noted (supplemental Figure 4).

Effect of ligands and cargoes on RBC function

Having characterized the binding of the antibody fragments and fusion proteins to human RBCs, we then investigated how the binding of these ligands may affect several parameters of RBC integrity including osmotic fragility, mechanical resistance, membrane deformability, exposure of PS, and generation of ROS. These experiments were conducted at 5% hematocrit and with ligand-to-RBC ratios calculated to yield 10 000 and 100 000 copies per RBC for both ligands based on their affinity and the known concentration of RBC targets. These copy numbers are below saturation for both Wr^b and Rh17.

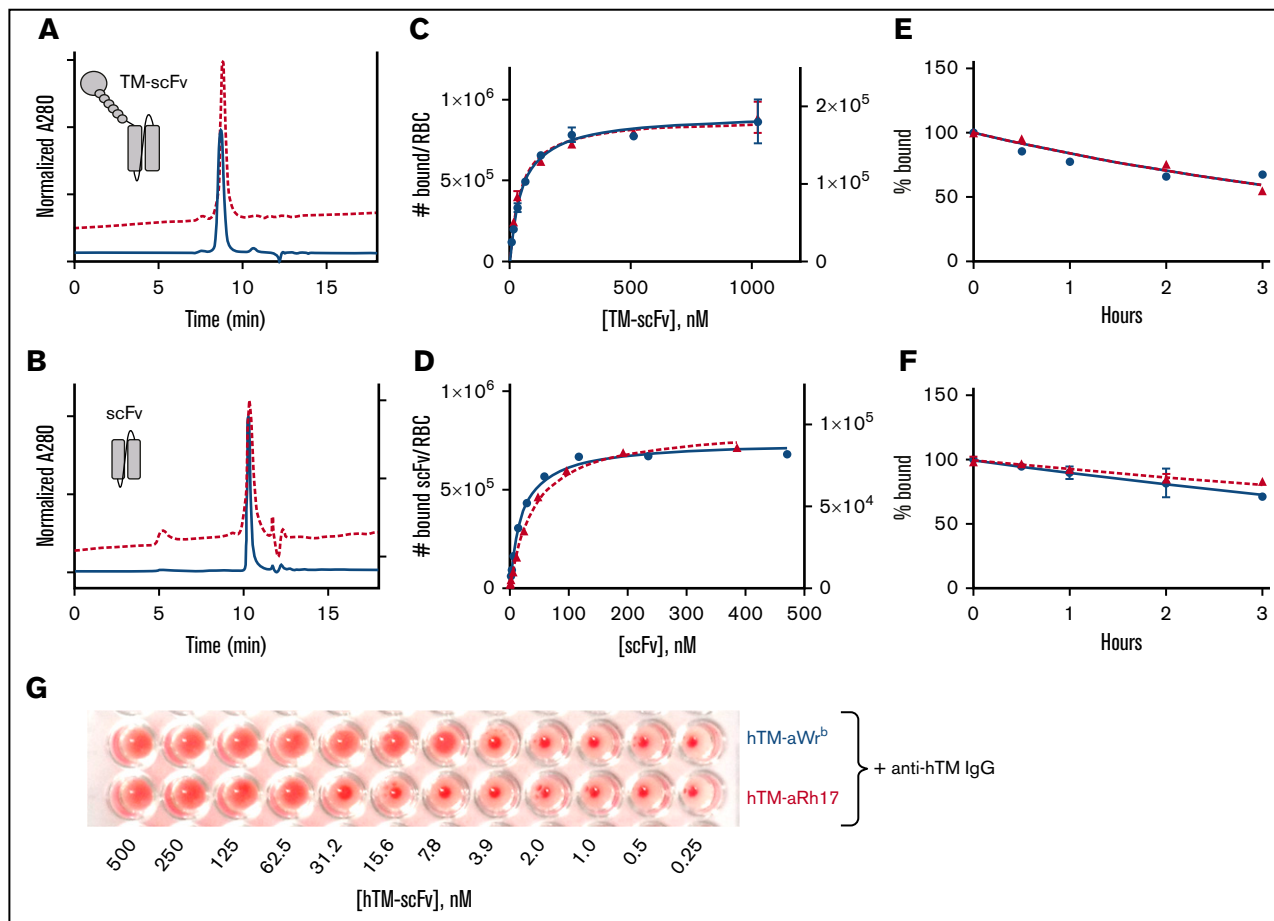


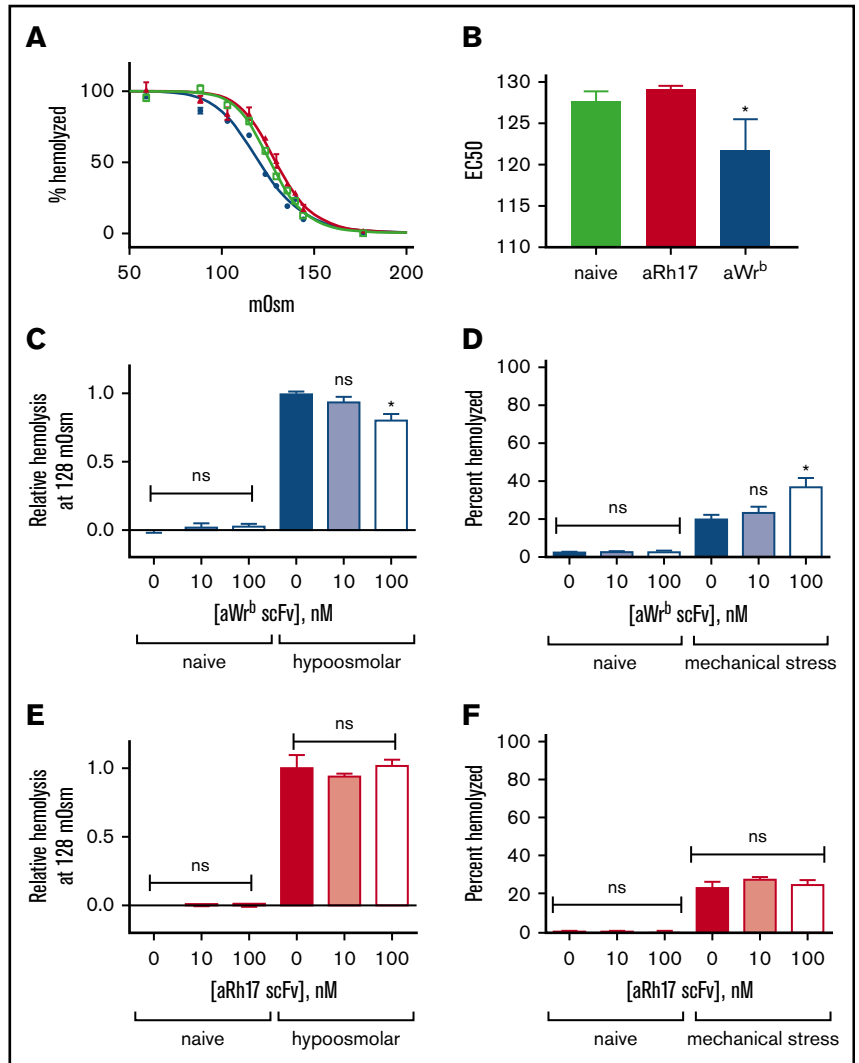
Figure 1. Characterization of aRh17 and aWr^b ligands and their binding to human RBCs. Representative size-exclusion HPLC analysis of (A) hTM-scFv fusions and (B) scFvs alone directed to band 3/GPA (aWr^b, solid blue lines) and RhCE (aRh17, dashed red lines) demonstrates high purity of recombinant proteins and elution times consistent with theoretical molecular weights. Direct binding assays with radiolabeled proteins demonstrates high affinity and B_{max} (supplemental Table 1) consistent with reported copy number of the surface targets for both the (C) hTM-scFv fusions and the (D) scFv antibodies. No significant nonspecific binding to control murine RBCs was seen. Representative data of 3 independent experiments are shown. Ligand dissociation studies demonstrated slow dissociation kinetics (>50% bound at 3 hours) for both the (E) TM-scFv fusions and (F) scFv antibodies. (G) Binding assay by hemagglutination techniques demonstrated that when anti-hTM IgG antibody (100 nM) was added to RBC prebound with the indicated concentration of hTM-scFv fusions, agglutination was observed when ~1000 copies of hTM would be expected on the surface. Representative data of 3 independent experiments are shown. No agglutination was seen with RBCs treated with either scFv or hTM-scFv alone or with mouse, rat, or pig RBCs treated with scFv or hTM-scFv followed by anti-hTM.

We found that the 2 scFvs (and their corresponding TM fusions) had significantly different effects on target RBCs. Targeting of Wr^b, but not Rh17, by the antibody fragments induced a left shift in osmotic fragility curves (50% effective concentration [EC₅₀] 122 vs 128 mOsm, $P < .05$) with a pattern suggesting a whole population change rather than just a subset (Figure 2A-B). We tested the dose dependence of the observed changes in osmotic resistance using the EC₅₀ of naive RBCs (128 mOsm) (Figure 2C, E) and again found that aRh17 did not produce changes in osmotic hemolysis at this osmolarity, whereas aWr^b again decreased hemolysis. The changes in osmotic resistance were paralleled by an increase in hemolysis following mechanical stress for aWr^b (Figure 2D), but similarly, no change was seen after treatment with aRh17 (Figure 2F). Although the mechanical stress assay⁴⁰ does not directly represent a pathophysiologic scenario, it is intended to reflect overall integrity of the RBC membrane architecture. Nearly identical effects were observed after treatment with the scFvs alone or with their corresponding TM fusions (Figure 3A-B).

We then used ektacytometry to test whether effects on osmotic and mechanical fragility were mirrored by alterations in membrane deformability. In this technique, a decrease in $E_{l_{max}}$ or an increase in SS1/2 reflects an increase in RBC rigidity. As we expected, when ligands were bound to Wr^b, there was a dose-dependent increase in RBC rigidity (Figure 4), reflected in both increased SS1/2 (Figure 4B, D) or decreased $E_{l_{max}}$ (supplemental Figure 5). This rigidifying effect was identical for TM-scFv fusions and scFvs alone, again demonstrating that the ligand, and not the TM cargo, induced these changes. Consistent with the mechanical and osmotic stress assays, binding of fusions or scFvs to RhCE did not change ektacytometric curves or indices (Figure 4) and the behavior of aRh17-treated RBCs was consistently identical to naive donor RBCs.

The target-dependent effect of these ligands on membrane deformability raised the question of how targeting other RBC epitopes (particularly on GPA, given its ubiquity as an erythroid-specific target) might affect RBC physiology. To probe this

Figure 2. aRh17 and aWr^b antibodies demonstrate differential effects on RBC resistance to osmotic and mechanical stress. Osmotic stress was induced by incubation in buffered (10 mM sodium phosphate) saline at a range of osmolalities (0-308 mOsm). Mechanical stress was induced by rotation in the presence of glass beads at 1% hematocrit (Hct). Antibodies were added at 10 nM and 100 nM to 5% Hct RBC suspension, which produces a ratio of $\sim 10^4$ and 10^5 ligands per RBC and is below saturation for both target antigens. (A) RBCs treated with 500 nM aWr^b scFv (blue) showed a left shift in the osmotic lysis curve compared with naive (green) or aRh17 scFv-treated RBCs (red). (B) RBCs treated with aWr^b but not aRh17 showed a significant change in the concentration required for 50% hemolysis (128 vs 120 mOsm, $n = 3$, $*P < .05$, 1-way analysis of variance [ANOVA] with Holm-Sidak correction for multiple comparisons). (C) aWr^b scFv-treated RBCs (blue) show a dose-dependent decrease in hemolysis in response to osmotic stress at 128 mOsm (EC50 for naive RBCs) and (D) a dose-dependent increase in hemolysis in response to mechanical stress. aRh17 scFv-treated RBCs (red) do not demonstrate any significant change in response to (E) osmotic stress or (F) mechanical stress. In all experiments, means \pm standard deviation (SD) are shown; $n = 3$ for each condition ($*P < .05$ compared with naive, 1-way ANOVA with Holm-Sidak correction for multiple comparisons). ns, not significant.



question, we produced anti-GPA antibodies and Fab fragments from a commercially available hybridoma, YTH89.1⁴⁶ (supplemental Figure 6). After incubating human RBCs with the anti-GPA IgG antibodies or their monovalent Fabs, we observed similar rigidifying effects to those seen with aWr^b ligands. Monovalent Fab induced a slight dose-dependent change in ektacytometric indices, whereas the parent antibody induced more marked changes in red cell rigidity (supplemental Figure 7). The Fab also induced a slight increase in hemolysis under mechanical stress, while also inducing a slight increase in hemolysis under hypo-osmolar conditions. Because prior studies loading drugs onto murine RBCs have largely relied on Ter119 or other GPA-associated ligands as the targeting agent, we also examined the effects of a scFv-TM fusion of this antibody on mouse RBCs.²⁰ As with targeting of human Wr^b or GPA, Ter119-TM fusions decreased deformability of murine RBCs (increased SS1/2, decreased Elmax) as a monovalent fusion protein (Ter119-mTM), and markedly so as the parent IgG antibody (supplemental Figure 8). As with the human ligands, these changes in deformability were accompanied by changes in susceptibility to osmotic and mechanical stress.

To address the generalizability of the observed deformability effects of the band 3, GPA, and RhCE ligands, we also compared the

ektacytometric effects of a range of full-length IgG antibodies covering different epitopes on these membrane targets. For this purpose, we used BRIC69 (anti-RHCE, mouse IgG1), BRAD2 (anti-D, human IgG1), BRAD3 (anti-D, human IgG3), FOG1 (anti-D, human IgG1), BIRMA84b (anti-Wr^b, mouse IgG3), BRIC14 (anti-Wr^b, mouse IgG2a), YTH89.1 (anti-GPA, rat IgG2b), BRIC256 (anti-GPA, mouse IgG1), and BRIC200 (anti-band 3, mouse IgG1). In agreement with prior studies,^{26-28,31} we found that all IgGs tested against epitopes on GPA and band 3 induced decreases in deformability, whereas antibodies to RhCE and RhD (on serologically confirmed RHD⁺ RBC donors) showed minimal change from naive RBCs (Figure 5A-C). Although all IgGs were added at a ratio of $\sim 10^4$ monoclonal antibodies (mAbs) per RBC (10 nM mAb in a 5% RBC suspension), differences in affinities of these clones are likely to result in different numbers of bound copies and, therefore, the relative degrees of rigidification as a function of bound copy numbers remained uncertain. To address this, we selected representative anti-RhCE (BRIC69) and anti-Wr^b (BRIC14) IgG antibodies and performed additional dose-titration experiments to show that when the anti-RhCE antibodies were added at ratios below saturation and which resulted in similar total numbers of bound IgG as anti-Wr^b antibodies (Figure 5D-F), no change in SS1/2

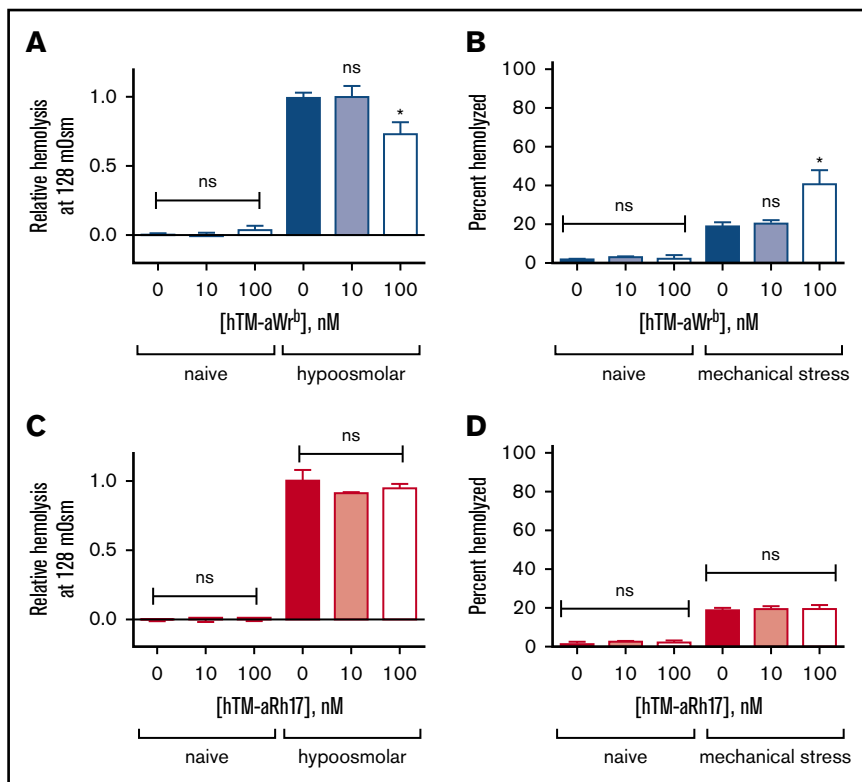


Figure 3. aRh17 and aWr^b hTM-scFv fusion proteins demonstrate similar patterns of changes in RBC resistance to osmotic and mechanical stress as the parent scFv. Fusion proteins were added at 10 nM and 100 nM to 5% Hct RBC suspension, which produces a ratio of $\sim 10^4$ and 10^5 fusion proteins per RBC and is below saturation for both target antigens. (A) aWr^b hTM-scFv shows a dose-dependent decrease in hemolysis in response to osmotic stress and (B) a dose-dependent increase in hemolysis in response to mechanical stress. aRh17 hTM-scFv does not demonstrate any significant change in response to (C) osmotic stress or (D) mechanical stress. In all experiments, means \pm SD are shown; $n = 3$ for each condition ($*P < .05$ compared with naive, 1-way ANOVA with Holm-Sidak correction for multiple comparisons).

was seen for anti-RhCE whereas anti-Wr^b showed significant, dose-dependent rigidification.

Additional characterization of the effects of the scFvs and fusions on RBCs included assays of PS surface exposure, as measured by annexin V binding and ROS generation. Binding of both scFvs and hTM-scFv fusions did not lead to a detectable increase in PS exposure (supplemental Figure 9A). None of the scFv ligands examined demonstrated detectable induction of ROS generation by a dihydrorhodamine-based assay (supplemental Figure 9B).

Therapeutic effectiveness of RBC cargoes

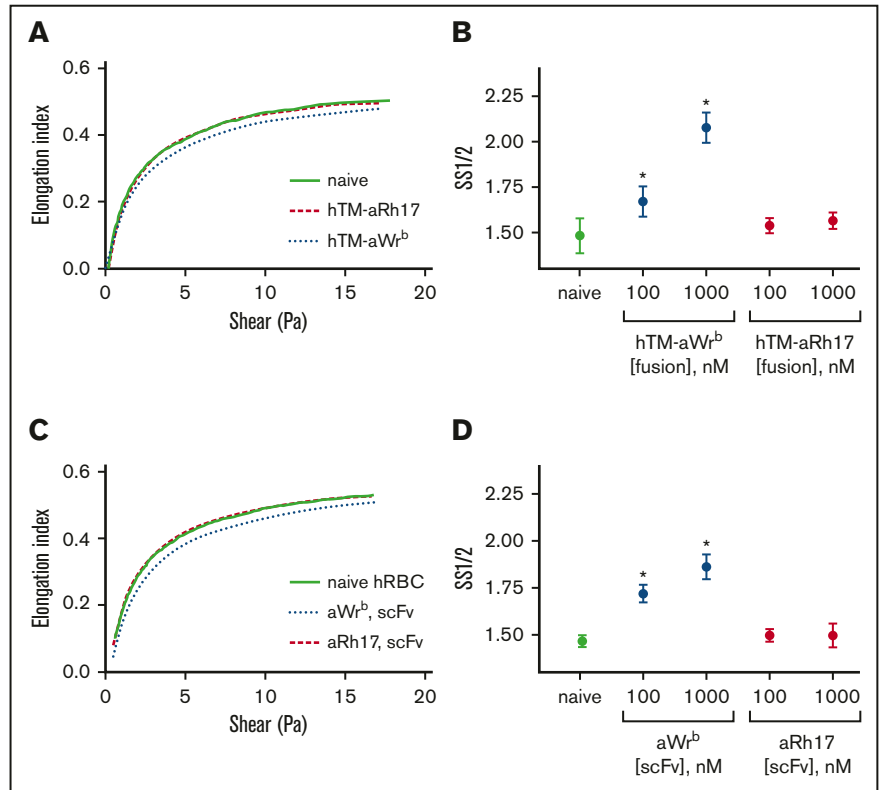
Having examined the effects on aWr^b and aRh17 scFvs and their respective TM fusion proteins on human RBC physiology, we next compared the enzymatic activity and therapeutic efficacy of these fusions. In solution, fusion proteins demonstrated activated protein C (APC)-generative capacity identical to soluble TM in the presence of human protein C and thrombin (supplemental Figure 10). Fusion proteins were then prebound to human RBCs at saturating concentrations and their capacity to generate APCs was measured as a function of RBC concentration. The fusions generated a RBC dose-dependent increase in APC generation by carrier RBCs (Figure 6A). Using a standard curve generated with soluble TM, the Wr^b-coupled RBC-TM generated roughly 100 000 soluble TM “equivalents” per loaded RBCs at saturation whereas the RhCE-coupled RBC-TM generated 50 000. Therefore, although Wr^b-coupled TM would be predicted to carry fivefold to 10-fold more copies of the fusion per RBC at saturation, the APC-generating capacity was only twofold higher. We then reversed these conditions such that RBCs and target epitopes were at excess (50 nM fusion in 20% hematocrit [Hct], ~ 10 000 copies per

RBCs), which would drive fusions to be essentially completely RBC-bound. At these high concentrations of RBCs, comparable to the circulatory environment, APC generation was similar for both fusion proteins and comparable to that seen for soluble TM, although a slight reduction was seen for hTM-aBand3/GPA and not hTM-aRhCE (Figure 6B). These results confirm that the fusions maintain their enzymatic activity when coupled to RBCs, and suggest that RhCE-coupled TM may better conserve specific activity.

We then tested the therapeutic activity of hTM/scFv fusions bound to human RBCs in a microfluidic model of microvascular inflammatory thrombosis that permits assessment of human-targeted therapeutics in whole blood in a system simulating human vessels.³⁷ In this model, fully endothelialized microchannels are activated with an inflammatory mediator (eg, TNF- α), inducing leukocyte and platelet adhesion and widespread fibrin generation when the channels are exposed to flowing human whole blood. We hypothesized that if the fusions maintain their activity in whole blood, they would significantly reduce fibrin and platelet deposition in response to inflamed endothelium. To test this, we added 200 nM of each fusion protein (and soluble TM as a control) to whole blood (a ratio of ~ 25 000 copies of TM per RBC at normal RBC counts). Both fusions significantly reduced fibrin deposition (measured by red fluorescence) in response to TNF- α activation (Figure 6C). Channels exposed to Wr^b-targeted TM fusions, as compared with RhCE-targeted, showed a slight increase in mostly platelet-associated fibrin deposition at the end of the perfusion period (20 minutes), but both remained significantly reduced compared with untreated controls and similar to soluble TM (supplemental Videos 1-4). Additional analysis of fluorescence from calcein AM labeling

Figure 4. aWr^b scFv and hTM-scFv increase RBC rigidity, whereas aRh17 scFv and hTM-scFv show no changes compared with naive RBCs.

Ektacytometry was performed on 5% Hct RBC suspensions incubated with scFv or hTM-scFv at the indicated concentrations. Elongation index (as calculated automatically by the instrument) was read as a function of shear stress, and nonlinear regression was used to calculate the shear stress required for half-maximal deformation and the Elmax. Representative curves of at least 3 independent experiments with different donors. (A) hTM-scFv fusions and (C) scFv antibodies targeted to band 3/GPA (aWr^b blue dotted lines) demonstrated a rightward shift in the ektacytometry curves compared with naive (solid line) whereas aRh17 fusions and scFv (red dashed lines) showed no change from naive (scFvs and fusion proteins added at 1000 nM). (B,D) The shift in deformability was quantified as the SS1/2, which showed dose-dependent increases in response to band 3/GPA-targeted ligands and not RhCE ligands. In panels B and D, mean ± SD is shown; n = 3-5 per condition (*P < .05 compared with naive, 1-way ANOVA with Holm-Sidak correction for multiple comparisons). hRBC, human RBC.



(leukocytes and platelets) demonstrated that RhCE-targeted hTM-scFv was more effective than the Wr^b-targeted fusion at reducing platelet and leukocyte adhesion (Figure 6D), with efficacy of hTM-aRhCE again similar to soluble TM. Hypothesizing that the increase in calcein signal in hTM-aWr^b compared with hTM-aRhCE was a result of rigidifying effects of the aWr^b, we performed additional experiments in this model using the aWr^b and aRhCE scFvs alone (not fused to TM), and demonstrated that after 15 minutes of flow, activated channels exposed to aWr^b scFv-treated blood showed greater platelet and leukocyte accumulation compared with that treated with aRh17 scFv (Figure 7), suggesting the difference in efficacy of hTM-aRhCE and hTM-aWr^b is due to aWr^b promotion of leukocyte and platelet adhesion rather than a loss of efficacy of the appended TM. We also confirmed that RBC rigidification was seen at this ratio of scFv to RBC in whole blood (supplemental Figure 9).

Discussion

As a critical step in the translation of RBC-targeted therapeutic fusion proteins to clinical practice, we designed human RBC-specific fusion proteins based on scFvs derived from nonhuman-primate antibody phage-display libraries. Using this technique, we generated antibodies against highly conserved, erythroid-specific epitopes on band 3/GPA (Wr^b) and RhCE (Rh17) proteins. Both epitopes are on multipass transmembrane proteins and exist predominantly within discrete multiprotein complexes. Although Wr^b is more widely distributed between band 3/ankrin complexes, junctional complexes, and free forms, Rh17 (as part of RhCE) exists largely within band/ankrin complexes.⁴⁷ Wr^b has been localized to a juxtamembrane site of interaction between GPA and band 3, but the precise epitope for Rh17, which is defined serologically, is

unknown. Both antibody fragments and their respective TM fusions showed affinities sufficient to drive rapid, complete binding in whole blood, where concentrations of their targets are > 1 μM. Although only a slight increase in off rate was noted for TM fusion proteins, interaction with TM-binding partners (thrombin, PF4, protein C) may promote dissociation in whole blood under flow, which was not directly assessed in the present study. The primate origin of these ligands is expected to confer less immunogenicity than nonengineered murine monoclonal antibodies or foreign peptides, but further data would be required to support this.

Targeting of band 3/GPA (Wr^b) led to changes in RBC membrane deformability, mechanical resistance, and osmotic resistance, whereas RhCE-targeted fusions and antibody fragments did not perturb any of the physiologic parameters assessed in this study. Membrane effects were shared, to varying extents, by other GPA and band 3 ligands against human and murine RBCs, including Ter119, particularly for bivalent IgG ligands. In contrast, antibodies against RhD and RhCE failed to demonstrate significant rigidification of human RBCs, consistent with prior literature.³¹ Antibodies against GPA and RhD can produce markedly different effects on different subsets of phagocytic cells,⁴⁸ and, although the authors hypothesized that copy number was critical, the current findings suggest that altered deformability may have also been contributory. The precise function of RhCE has been difficult to define⁴⁹ and a large diversity of polymorphisms has been described.⁴³ Individuals expressing RhD but not RhCE (rare D⁻ phenotype) show modest alteration of membranes without overt RBC or clinical phenotypes.⁵⁰ Although homologous proteins participate in ammonia/ammonium transport and acid/base balance, RhCE and RhD do not.^{51,52} Band 3 and GPA are highly

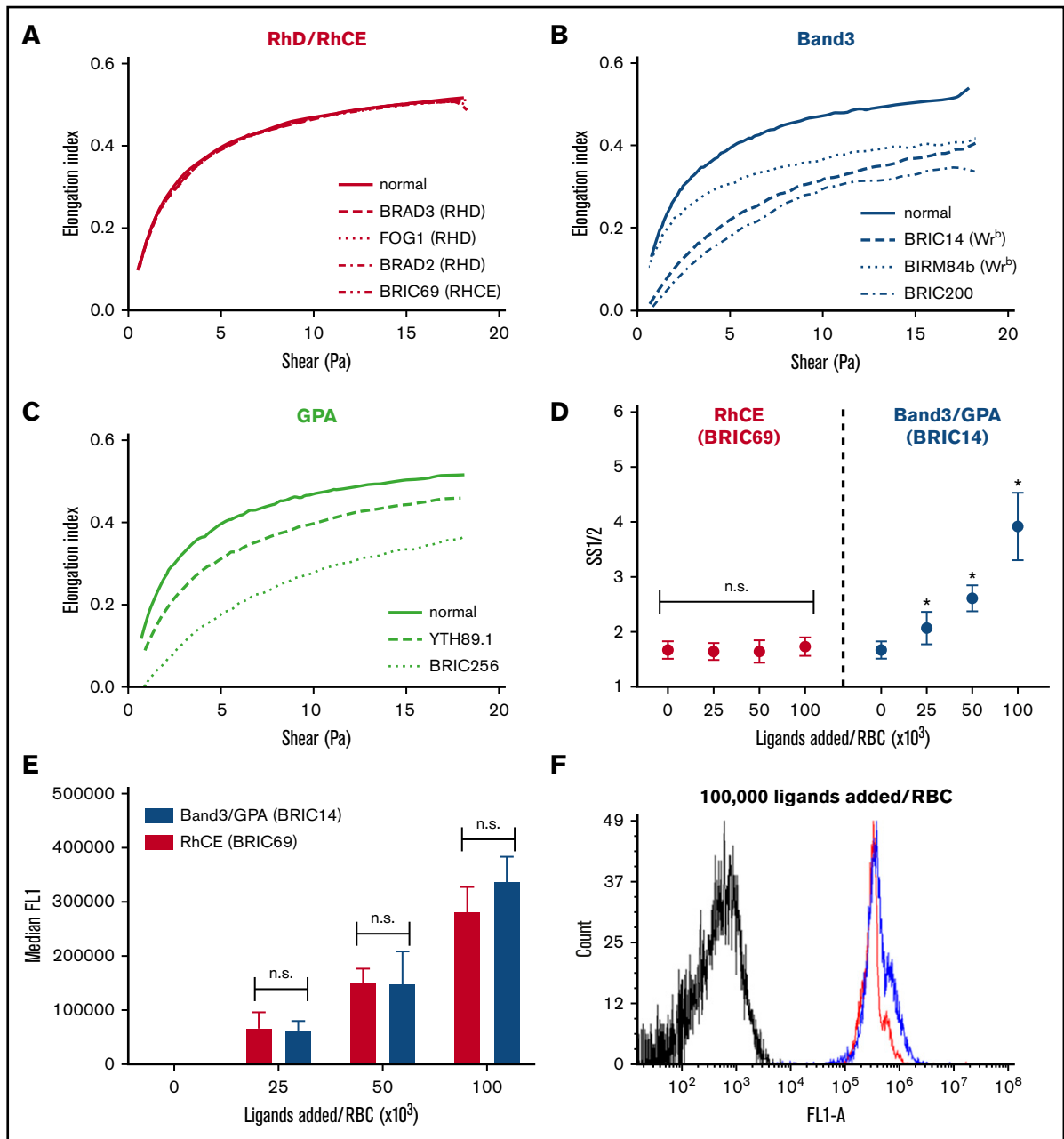


Figure 5. IgG antibodies against band 3 and GPA rigidify RBCs, whereas IgGs against RhCE and RhD do not. Representative ektacytometric curves (at least 3 separate donors studied per antibody) of RBCs treated with antibodies targeting (A) RhD or RhCE, (B) band 3 or W_r^b , or (C) GPA. A 5% suspension of RhD⁺ human RBCs in PBS was treated with 100 nM of the indicated antibody clones (~100 000 IgG per RBC). After incubation for 1 hour at 37°C, the red cell suspensions were read on an ektacytometer in 5.5% polyvinylpyrrolidone. Figure keys indicate antibody clones. (D) Ektacytometric dose response of anti-RhCE vs anti- W_r^b IgG antibodies. Selected antibody clones against RhCE (BRIC69, red) and W_r^b (BRIC14, blue) were added at 100 nM to varying hematocrit RBC suspensions (5%, 10%, and 20%, 6 donors tested) to result in ligand ratios of 25 000 to 100 000 IgG per RBC. a W_r^b demonstrated a significant increase in SS1/2 at all ligand-loading ratios, whereas no significant difference was seen for aRhCE antibodies. Mean \pm SD is shown, n = 3-6 for each condition. (E) Flow cytometry on aRhCE (BRIC69, red) and a W_r^b (BRIC14, blue) IgG-treated RBCs stained with Alexa Fluor 488–labeled anti-mouse secondary antibodies shows no significant difference in bound IgGs (based on median fluorescence) at the indicated loading ratios. (F) Representative histogram demonstrating similar antibody loading for RBCs treated with aRhCE (BRIC69, red) and a W_r^b (BRIC14, blue) antibodies.

expressed membrane proteins important for structural membrane complexes and ion exchange, and carriage of sialoglycoproteins, respectively. In this context, the apparent “unresponsiveness” of RBCs bound by RhD/RhCE-targeted ligands is consistent with a lack of recognized function in mature RBCs.

As a representative therapeutic, we coupled TM to both scFvs. TM shows promise in the treatment of sepsis,⁵³ and RBC-coupled TM has demonstrated superiority to soluble TM in mouse models.^{20,21} Coupling TM to either epitope resulted in efficacious RBC drug carriers as measured by enzymatic activity and in a humanized

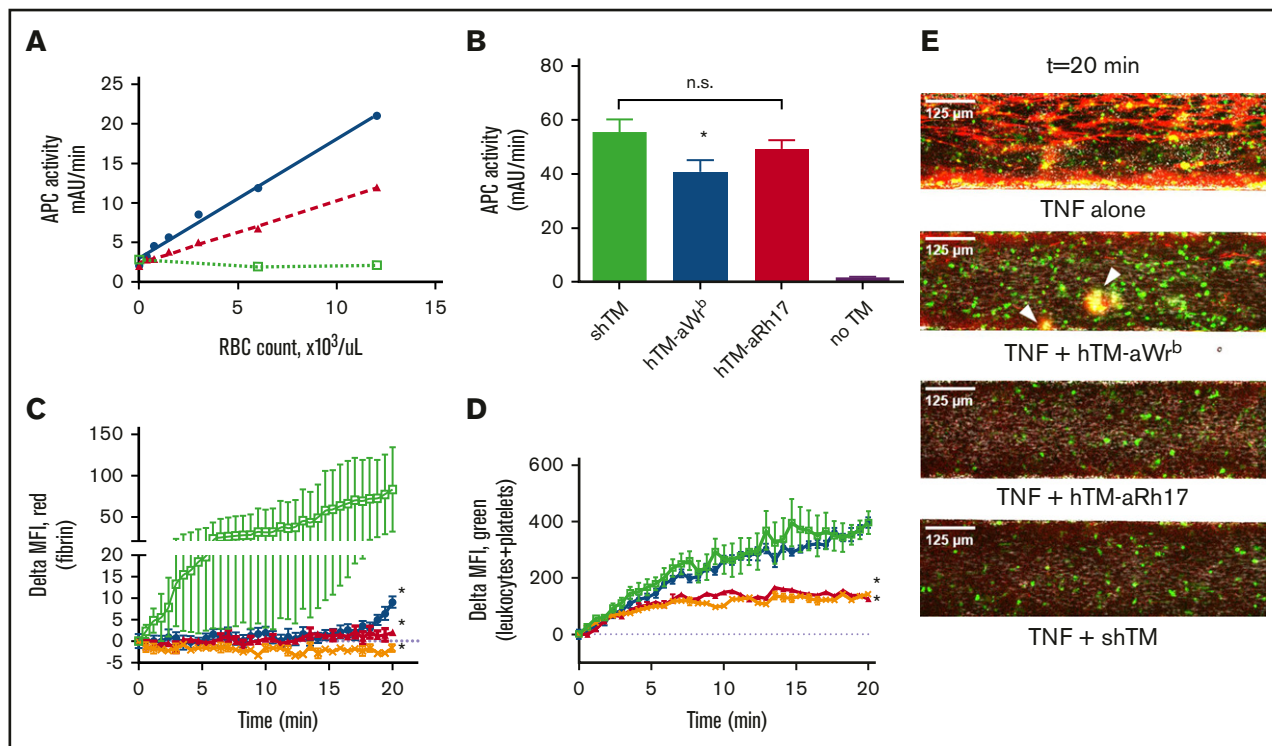


Figure 6. Characterization of the activity of RBCs bound by hTM-scFv fusions and their therapeutic efficacy in a microfluidic model of inflammatory thrombosis. (A) APC generation by RBCs loaded with hTM-scFv demonstrates a dose- and copy-number-dependent response in APC generation as measured by chromogenic assay. hTM-aBand3 (blue circles) showed about twofold higher APC generation per RBC compared with hTM-aRhCE (red triangles), although copy numbers are expected to be fivefold to tenfold higher. Soluble hTM (shTM)-treated RBCs are shown as a nonbinding control (green open squares). (B) Comparison of APC-generative capacity of sTM vs hTM-scFv fusions (added at 50 nM) in a high Hct (20%) RBC suspension. Mean \pm SD is shown; $n = 3$ for each condition ($*P < .05$ vs sTM, 1-way ANOVA with Holm-Sidak correction for multiple comparisons). A slight reduction in activity was seen for hTM-aBand3 but not hTM-aRhCE. (C) Fibrin generation on TNF- α -activated, endothelialized microfluidic channels perfused with human whole blood preincubated with either PBS control (green open squares), shTM control (orange crosses), hTM-aWr^b (blue circles), or hTM-aRh17 (red triangles). Both fusion proteins (and shTM⁺ control) significantly reduced fibrin generation ($*P < .05$ vs untreated, 1-way ANOVA with Holm-Sidak correction for multiple comparisons) as compared with the control channel. An increase in fibrin generation was noted toward the end of the observation period for the hTM-aWr^b-treated channels. (D) hTM-aRh17 treatment (red triangles) more effectively reduced platelet and leukocyte adhesion (quantified with calcein AM fluorescence) than hTM-aWr^b (blue circles) vs untreated control (open squares). hTM-Rh17 treatment was similar to shTM⁺ control (crosses). For panels C-D, mean \pm standard error of the mean (SEM) for 2 independent channels is shown. (E) Representative composite images of whole blood (fibrin in red [anti-fibrin-AlexaFluor568 stain], platelets and leukocytes in green [calcein AM stain], brightfield image in gray) flowing through endothelialized channels at the end of the observation period ($t = 20$ minutes). Fibrin is decreased in both fusion-treated channels. An increase in platelet adhesion with associated fibrin (yellow, arrowhead) is seen in the hTM-aWr^b-treated channels compared with hTM-aRh17 (see supplemental Videos 1-4 for the full time course).

microfluidic model of inflammatory thrombosis. However, RhCE-coupled TM showed higher specific activity *in vitro* and improved efficacy in our microfluidic model. The reasons for the difference in enzymatic activity may reflect spatial localization, as the Wr^b epitope is immediately adjacent to the RBC membrane, which may limit substrate accessibility, whereas the precise Rh17 epitope localization is unknown. The difference in efficacy in our humanized microfluidic model was unexpected, but because cellular rigidity has significant effects on margination of red cells, white cells, and platelets within the vascular lumen, and decreased RBC deformability can drive increased platelet adhesion,^{54,55} we speculate that the difference in efficacy reflects the observed difference in membrane effects. Our observation of higher platelet adhesion after treatment with Wr^b-targeted scFv is consistent with this phenomenon. The potential for drug or antibody loading of RBCs to affect their intravascular distribution and margination of cellular components, and how this distribution affects their therapeutic efficacy, warrants further investigation.

RBCs can respond to their environment in diverse ways including dynamic changes in linkage of membrane protein complexes,⁵⁶ phosphorylation of membrane and cytoskeletal components,⁵⁷⁻⁶⁰ calcium influx,^{61,62} PS exposure,^{29,63} and oxidative stress responses.³⁰ In targeting RBCs for delivery of therapeutics, the present findings suggest that dose- and target-dependent changes in membrane physiology, and ultimately, circulatory behavior should be carefully considered.^{24-29,64} As increases in RBC rigidity can result in an override of the CD47/SIRPA interaction,⁶⁵ these factors may also play a role in RBC interactions with host defenses and immune response. This is especially important because RBC drug carriers are drawing increased attention for their apparent ability to modulate immune responses and even induce immune tolerance.¹³⁻¹⁵ However, although ligands to murine RBCs have been explored (eg, Ter119, ERY1) in this approach, application to human RBCs has not been well developed.

Based on the current findings, RhCE (on Rh17) may be a particularly attractive target for surface loading of RBCs given its

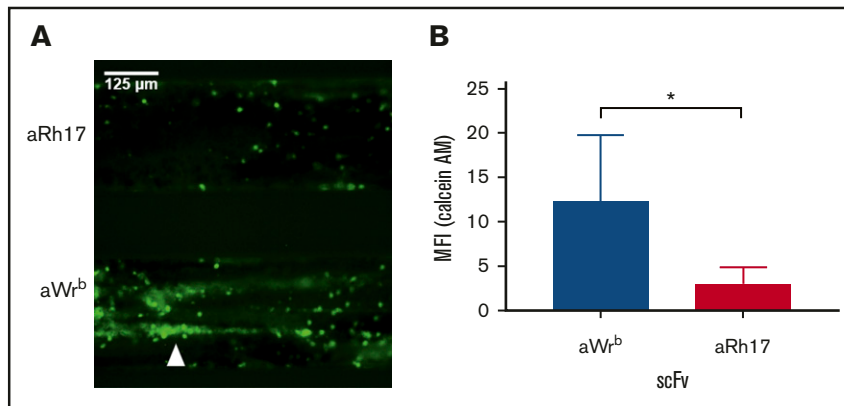


Figure 7. Whole blood treated with aWr^b scFv shows increased platelet adhesion in response to flow over TNF- α -activated endothelium compared with blood treated with aRh17. (A) Representative image of endothelialized channels subjected to flow with either (top) aWr^b scFv treated whole blood or (bottom) aRh17 scFv treated whole blood. Blood was collected in citrate with corn trypsin inhibitor, incubated with scFv (500 nM) for 15 minutes, recalcified, and flowed over channels for 15 minutes after which images were captured across the channels. Prior to flow, platelets and leukocytes were stained by addition of calcein AM dye. (B) Quantification of the experiments in panel A (mean fluorescence intensity) demonstrates a significant increase in calcein AM signal in the aWr^b scFv-treated blood but not aRh17 scFv ($n = 4$, $*P < .05$, 1-way ANOVA).

erythroid specificity, high copy number, apparent lack of adverse impact on RBC physiology, and presence on the RBCs of essentially 100% of the human population. The therapeutic efficacy of hTM targeted to human RBCs on either epitope was comparable to soluble TM, and was optimal when coupled to RhCE. The ligands described in the present study offer a new set of biochemical tools for optimizing the delivery of therapeutics by human RBCs.

Acknowledgments

The authors acknowledge members of the blood bank at the Hospital of the University of Pennsylvania for providing antibody reagents as well as RBCs from donor units. The authors also acknowledge Marion Reid at the New York Blood Center for contributions to identification of antibody target antigens, Antoine Blancher for contributions to macaque immunization, and Sergei Zaitsev for providing the S2 cell line used for production of Ter119-mTM.

This work was supported by National Institutes of Health, National Heart, Lung, and Blood Institute grants 5R01HL121134-03, 5P01HL40387, and 5T32HL007775-23.

REFERENCES

1. Ihler GM, Glew RH, Schnure FW. Enzyme loading of erythrocytes. *Proc Natl Acad Sci USA*. 1973;70(9):2663-2666.
2. Ihler G, Lantzy A, Purpura J, Glew RH. Enzymatic degradation of uric acid by uricase-loaded human erythrocytes. *J Clin Invest*. 1975;56(3):595-602.
3. Wakamiya RT, Lightfoot EN, Updike SJ. Asparaginase entrapped in red blood cells: action and survival. *Science*. 1976;193(4254):681-683.
4. Bourgeaux V, Lanao JM, Bax BE, Godfrin Y. Drug-loaded erythrocytes: on the road toward marketing approval. *Drug Des Devel Ther*. 2016;10:665-676.
5. Villa CH, Cines DB, Siegel DL, Muzykantov V. Erythrocytes as carriers for drug delivery in blood transfusion and beyond. *Transfus Med Rev*. 2017;31(1):26-35.
6. Magnani M. Erythrocytes as carriers for drugs: the transition from the laboratory to the clinic is approaching. *Expert Opin Biol Ther*. 2012;12(2):137-138.
7. Leuzzi V, Micheli R, D'Agnano D, et al. Positive effect of erythrocyte-delivered dexamethasone in ataxia-telangiectasia. *Neurol Neuroimmunol Neuroinflamm*. 2015;2(3):e98.
8. Hunault-Berger M, Leguay T, Hugué F, et al; Group for Research on Adult Acute Lymphoblastic Leukemia (GRAALL). A Phase 2 study of L-asparaginase encapsulated in erythrocytes in elderly patients with Philadelphia chromosome negative acute lymphoblastic leukemia: the GRASPALL/GRAALL-SA2-2008 study. *Am J Hematol*. 2015;90(9):811-818.

Authorship

Contribution: C.H.V., D.C.P., C.F.G., L.R.W., and E.D.H. designed and performed experiments including recombinant protein production and modification, binding studies, and RBC functional studies; C.H.V. wrote the manuscript; C.H.V., I.H.J., and C.F.G. designed and performed microfluidic experiments; D.L.S. performed antibody phage-display experiments, characterized antibodies, designed experiments, and edited the manuscript; and D.B.C., M.P., and V.R.M. assisted with experimental design and edited the manuscript.

Conflict-of-interest disclosure: V.R.M. serves on the scientific advisory board of Anokion SA. V.R.M., D.L.S., and C.H.V. have filed for intellectual property on patents related to the technologies described in the study. The remaining authors declare no competing financial interests.

Correspondence: Vladimir R. Muzykantov, Perelman School of Medicine, University of Pennsylvania, STRC 10-178, 3400 Civic Center Blvd, Building 421, Philadelphia, PA 19104-5158; e-mail: muzykant@mail.med.upenn.edu.

9. Kontos S, Hubbell JA. Improving protein pharmacokinetics by engineering erythrocyte affinity. *Mol Pharm.* 2010;7(6):2141-2147.
10. Zaitsev S, Spitzer D, Murciano JC, et al. Sustained thromboprophylaxis mediated by an RBC-targeted pro-urokinase zymogen activated at the site of clot formation. *Blood.* 2010;115(25):5241-5248.
11. Shi J, Kundrat L, Pishesha N, et al. Engineered red blood cells as carriers for systemic delivery of a wide array of functional probes. *Proc Natl Acad Sci USA.* 2014;111(28):10131-10136.
12. Fesnak AD, June CH, Levine BL. Engineered T cells: the promise and challenges of cancer immunotherapy. *Nat Rev Cancer.* 2016;16(9):566-581.
13. Kontos S, Kourtis IC, Dane KY, Hubbell JA. Engineering antigens for in situ erythrocyte binding induces T-cell deletion. *Proc Natl Acad Sci USA.* 2013;110(1):E60-E68.
14. Grimm AJ, Kontos S, Diaceri G, Quaglia-Thermes X, Hubbell JA. Memory of tolerance and induction of regulatory T cells by erythrocyte-targeted antigens. *Sci Rep.* 2015;5(1):15907.
15. Lorentz KM, Kontos S, Diaceri G, Henry H, Hubbell JA. Engineered binding to erythrocytes induces immunological tolerance to *E. coli* asparaginase. *Sci Adv.* 2015;1(6):e1500112.
16. Villa CH, Pan DC, Zaitsev S, Cines DB, Siegel DL, Muzykantor VR. Delivery of drugs bound to erythrocytes: new avenues for an old intravascular carrier. *Ther Deliv.* 2015;6(7):795-826.
17. Murciano JC, Medinilla S, Eslin D, Atochina E, Cines DB, Muzykantor VR. Prophylactic fibrinolysis through selective dissolution of nascent clots by tPA-carrying erythrocytes. *Nat Biotechnol.* 2003;21(8):891-896.
18. Ganguly K, Krasik T, Medinilla S, et al. Blood clearance and activity of erythrocyte-coupled fibrinolytics. *J Pharmacol Exp Ther.* 2005;312(3):1106-1113.
19. Gersh KC, Zaitsev S, Cines DB, Muzykantor V, Weisel JW. Flow-dependent channel formation in clots by an erythrocyte-bound fibrinolytic agent. *Blood.* 2011;117(18):4964-4967.
20. Zaitsev S, Kowalska MA, Neyman M, et al. Targeting recombinant thrombomodulin fusion protein to red blood cells provides multifaceted thromboprophylaxis. *Blood.* 2012;119(20):4779-4785.
21. Carnemolla R, Villa CH, Greineder CF, et al. Targeting thrombomodulin to circulating red blood cells augments its protective effects in models of endotoxemia and ischemia-reperfusion injury. *FASEB J.* 2017;31(2):761-770.
22. Kina T, Ikuta K, Takayama E, et al. The monoclonal antibody TER-119 recognizes a molecule associated with glycophorin A and specifically marks the late stages of murine erythroid lineage. *Br J Haematol.* 2000;109(2):280-287.
23. Sahoo K, Koralege RS, Flynn N, et al. Nanoparticle attachment to erythrocyte via the glycophorin A targeted ERY1 ligand enhances binding without impacting cellular function. *Pharm Res.* 2016;33(5):1191-1203.
24. Knowles DW, Chasis JA, Evans EA, Mohandas N. Cooperative action between band 3 and glycophorin A in human erythrocytes: immobilization of band 3 induced by antibodies to glycophorin A. *Biophys J.* 1994;66(5):1726-1732.
25. Pasvol G, Chasis JA, Mohandas N, Anstee DJ, Tanner MJ, Merry AH. Inhibition of malarial parasite invasion by monoclonal antibodies against glycophorin A correlates with reduction in red cell membrane deformability. *Blood.* 1989;74(5):1836-1843.
26. Chasis JA, Reid ME, Jensen RH, Mohandas N. Signal transduction by glycophorin A: role of extracellular and cytoplasmic domains in a modulatable process. *J Cell Biol.* 1988;107(4):1351-1357.
27. Chasis JA, Mohandas N, Shohet SB. Erythrocyte membrane rigidity induced by glycophorin A-ligand interaction. Evidence for a ligand-induced association between glycophorin A and skeletal proteins. *J Clin Invest.* 1985;75(6):1919-1926.
28. Paulitschke M, Nash GB, Anstee DJ, Tanner MJ, Gratzer WB. Perturbation of red blood cell membrane rigidity by extracellular ligands. *Blood.* 1995;86(1):342-348.
29. Head DJ, Lee ZE, Swallah MM, Avent ND. Ligation of CD47 mediates phosphatidylserine expression on erythrocytes and a concomitant loss of viability in vitro. *Br J Haematol.* 2005;130(5):788-790.
30. Khoory J, Estanislau J, Elkhal A, et al. Ligation of glycophorin A generates reactive oxygen species leading to decreased red blood cell function. *PLoS One.* 2016;11(1):e0141206.
31. Ballas SK, Mohandas N, Clark MR, Shohet SB. Rheological properties of antibody-coated red cells. *Transfusion.* 1984;24(2):124-129.
32. Lizcano A, Secundino I, Döhrmann S, et al. Erythrocyte sialoglycoproteins engage Siglec-9 on neutrophils to suppress activation. *Blood.* 2017;129(23):3100-3110.
33. Schofield AE, Reardon DM, Tanner MJ. Defective anion transport activity of the abnormal band 3 in hereditary ovalocytic red blood cells. *Nature.* 1992;355(6363):836-838.
34. Rojewski MT, Schrezenmeier H, Flegel WA. Tissue distribution of blood group membrane proteins beyond red cells: evidence from cDNA libraries. *Transfus Apheresis Sci.* 2006;35(1):71-82.
35. Blancher A, Roubinet F, Reid ME, Socha WW, Bailly P, Bénard P. Characterization of a macaque anti-Rh17-like monoclonal antibody. *Vox Sang.* 1998;75(1):58-62.
36. Bruce LJ, Ring SM, Anstee DJ, Reid ME, Wilkinson S, Tanner MJ. Changes in the blood group Wright antigens are associated with a mutation at amino acid 658 in human erythrocyte band 3: a site of interaction between band 3 and glycophorin A under certain conditions. *Blood.* 1995;85(2):541-547.
37. Greineder CF, Johnston IH, Villa CH, et al. ICAM-1-targeted thrombomodulin mitigates tissue factor-driven inflammatory thrombosis in a human endothelialized microfluidic model. *Blood Adv.* 2017;1(18):1452-1465.

38. Siegel DL, Reid ME, Lee H, Blancher A. Scientific section. *Transfusion*. 1999;39(S10):1S-123S.
39. Roback JD. Technical Manual. Bethesda, MD: American Association of Blood Banks; 2014.
40. Pan D, Vargas-Morales O, Zern B, et al. The effect of polymeric nanoparticles on biocompatibility of carrier red blood cells. *PLoS One*. 2016;11(3):e0152074.
41. Baskurt OK, Meiselman HJ. Data reduction methods for ektacytometry in clinical hemorheology. *Clin Hemorheol Microcirc*. 2013;54(1):99-107.
42. Huang CH, Reid ME, Xie SS, Blumenfeld OO. Human red blood cell Wright antigens: a genetic and evolutionary perspective on glycophorin A-band 3 interaction. *Blood*. 1996;87(9):3942-3947.
43. Chou ST, Westhoff CM. The Rh and RhAG blood group systems. *Immunohematology*. 2010;26(4):178-186.
44. Gao SH, Huang K, Tu H, Adler AS. Monoclonal antibody humanness score and its applications. *BMC Biotechnol*. 2013;13(1):55.
45. Lomas-Francis C, Olsson ML. The Blood Group Antigen Factsbook. Cambridge, MA: Elsevier/Academic Press; 2012.
46. Jokiranta TS, Meri S. Biotinylation of monoclonal antibodies prevents their ability to activate the classical pathway of complement. *J Immunol*. 1993; 151(4):2124-2131.
47. Burton NM, Bruce LJ. Modelling the structure of the red cell membrane. *Biochem Cell Biol*. 2011;89(2):200-215.
48. Meinderts SM, Oldenburg P-A, Beuger BM, et al. Human and murine splenic neutrophils are potent phagocytes of IgG-opsonized red blood cells. *Blood Adv*. 2017;1(14):875-886.
49. Westhoff CM. Deciphering the function of the Rh family of proteins. *Transfusion*. 2005;45(suppl 2):117S-121S.
50. Flatt JF, Musa RH, Ayob Y, et al. Study of the D- phenotype reveals erythrocyte membrane alterations in the absence of RHCE. *Br J Haematol*. 2012; 158(2):262-273.
51. Ripoche P, Bertrand O, Gane P, Birkenmeier C, Colin Y, Cartron JP. Human rhesus-associated glycoprotein mediates facilitated transport of NH(3) into red blood cells. *Proc Natl Acad Sci USA*. 2004;101(49):17222-17227.
52. Gruswitz F, Chaudhary S, Ho JD, et al. Function of human Rh based on structure of RhCG at 2.1 A. *Proc Natl Acad Sci USA*. 2010;107(21):9638-9643.
53. Levi M. Recombinant soluble thrombomodulin: coagulation takes another chance to reduce sepsis mortality. *J Thromb Haemost*. 2015;13(4):505-507.
54. Fay ME, Myers DR, Kumar A, et al. Cellular softening mediates leukocyte demargination and trafficking, thereby increasing clinical blood counts. *Proc Natl Acad Sci USA*. 2016;113(8):1987-1992.
55. Watts T, Barigou M, Nash GB. Comparative rheology of the adhesion of platelets and leukocytes from flowing blood: why are platelets so small? *Am J Physiol Heart Circ Physiol*. 2013;304(11):H1483-H1494.
56. Chu H, McKenna MM, Krump NA, et al. Reversible binding of hemoglobin to band 3 constitutes the molecular switch that mediates O₂ regulation of erythrocyte properties. *Blood*. 2016;128(23):2708-2716.
57. Kalfa TA, Pushkaran S, Mohandas N, et al. Rac GTPases regulate the morphology and deformability of the erythrocyte cytoskeleton. *Blood*. 2006; 108(12):3637-3645.
58. Wautier MP, El Nemer W, Gane P, et al. Increased adhesion to endothelial cells of erythrocytes from patients with polycythemia vera is mediated by laminin alpha5 chain and Lu/BCAM. *Blood*. 2007;110(3):894-901.
59. Glodek AM, Mirchev R, Golan DE, et al. Ligation of complement receptor 1 increases erythrocyte membrane deformability. *Blood*. 2010;116(26): 6063-6071.
60. Ferru E, Giger K, Pantaleo A, et al. Regulation of membrane-cytoskeletal interactions by tyrosine phosphorylation of erythrocyte band 3. *Blood*. 2011; 117(22):5998-6006.
61. Brody JP, Han Y, Austin RH, Bitensky M. Deformation and flow of red blood cells in a synthetic lattice: evidence for an active cytoskeleton. *Biophys J*. 1995;68(6):2224-2232.
62. Shields M, La Celle P, Waugh RE, Scholz M, Peters R, Passow H. Effects of intracellular Ca²⁺ and proteolytic digestion of the membrane skeleton on the mechanical properties of the red blood cell membrane. *Biochim Biophys Acta*. 1987;905(1):181-194.
63. Nguyen DB, Wagner-Britz L, Maia S, et al. Regulation of phosphatidylserine exposure in red blood cells. *Cell Physiol Biochem*. 2011;28(5):847-856.
64. Head DJ, Lee ZE, Poole J, Avent ND. Expression of phosphatidylserine (PS) on wild-type and Gerbich variant erythrocytes following glycophorin-C (GPC) ligation. *Br J Haematol*. 2005;129(1):130-137.
65. Sosale NG, Rouhiparkouhi T, Bradshaw AM, Dimova R, Lipowsky R, Discher DE. Cell rigidity and shape override CD47's "self"-signaling in phagocytosis by hyperactivating myosin-II. *Blood*. 2015;125(3):542-552. <https://doi.org/10.1182/blood-2014-06-585299>